



Real-time FTIR monitoring of the photopolymerization of a pentaerythritol triacrylate-based resin

Abderrazek Oueslati^a, Saber Kamoun^{a‡}, Faouzi Hlel^a, Mohamed Gargouri^a, Alain Fort^b

^a *Laboratoire de l'état solide, Département de physique, Faculté des Sciences de Sfax, BP 802, 3018, Tunisie*

^b *Institut de physique et chimie de Strasbourg, IPMS, UMR 7504, France*

Real-time dielectric and infrared measurements were performed to follow the photopolymerization reaction of a pentaerythritol triacrylate-based resin. Monomer and polymer conversions were followed by Fourier transform infrared spectroscopy (FTIR). Changes in charge carrier mobility were analyzed by dielectric relaxation spectroscopy. The measurements were made over a range of frequencies between 2 and 10^7 Hz, with irradiation times varying from 4 to 84 minutes. The complex electric functions impedance (Z^*), complex modulus (M^*) and conductivity, were used to investigate the relaxation processes. A Cole–Cole model was used to analyze the relaxation parameters and the distribution of relaxation time.

KEYWORDS: Photopolymerization; FTIR; impedance spectroscopy

COPYRIGHT: © 2011 Oueslati et al. This is an open-access article distributed under the terms of the Creative Commons Attribution License, which permits unrestricted use, distribution, and reproduction in any medium, provided the original author and source are credited.

Polymers with reactive groups are widely used for coupling reactions with functional compounds with valuable properties such as catalytic activities, biological activities and electro-optical properties [1]. *In situ* real-time monitoring of chemical and physical changes during processing of reactive polymer-forming materials is of crucial importance to scientists and engineers [2]. Many dielectric studies of photopolymerizable resin systems have been reported, with several groups trying to relate the changes in dielectric properties to chemical and physical phenomena that occur during the reaction [3-6]. The study of the evolution of the dielectric

properties of a system undergoing a photopolymerization reaction requires a suitable technique for monitoring *in situ* polymeric material processing [7]. However, it has become apparent that these studies are also able to provide a better understanding of the molecular dynamics and diffusion processes in these systems [8-12]: Electrical spectroscopy of a photopolymerization medium measures the total response of changes of mobility of various dipole species and ions, which contribute to real and imaginary parts of the electrical constant on different time scales of electrical spectra. The evaluation of the complex electrical parameters (impedance Z^* , complex modulus M^* , conductivity) as functions of frequency permit detection of the presence of relaxation processes in the photopolymerizable resin. In this work, we investigate infrared and electrical properties during photopolymerization.

[‡]Correspondence: S. Kamoun@yahoo.fr

Received: 02 October 2010; Accepted: 01 December 2010

Methods

The photopolymerizable resin used in this study was a mixture of three basic components: a sensitizer dye Eosin Y (2', 4', 5', 7'- tetrabromofluorescein disodium salt, 0.1% w/v, **fig. 1a**), a cosensitizer N-methyldiethanolamine (MDEA, 5% w/v, **fig. 1b**), and a multifunctional acrylate monomer pentaerythritol triacrylate (PETIA, **fig. 1c**) which was the solvent of the two other reactants. The *in situ* photopolymerization experiment was carried out using a 50W halogen lamp. Samples maintained contact with air during irradiation. The infrared spectrum was recorded in the 400 – 4000 cm^{-1} range using a Perkin-Elmer FT-IR 1000 spectrometer, using samples pressed in spectroscopically pure KBr pellets. Impedance spectroscopy was performed using pellet discs of about 12 mm in diameter and 1.05 mm in thickness, and measured with a Novo Control apparatus working in the frequency range 2 -

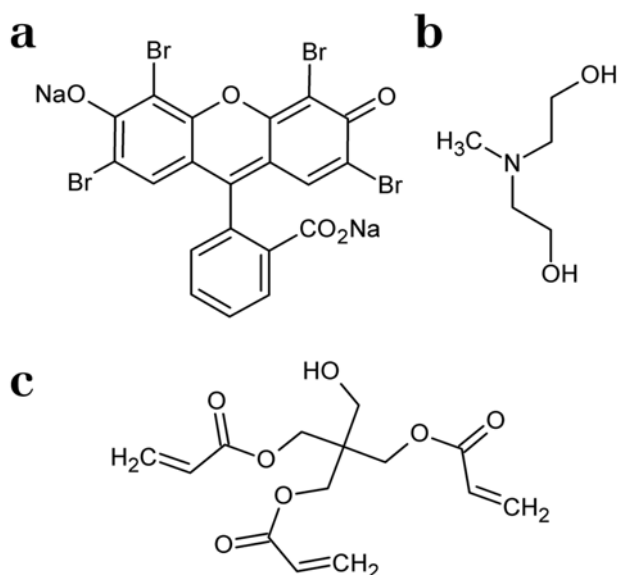


Figure 1. Molecular structures of the different components of the photopolymerizable resin: (a) Eosin Y, (b) MDEA and (c) PETIA

10^7 Hz.

Results and Discussion

Infrared absorption spectroscopy

The infrared spectrum of the photopolymerizable resin obtained after 20 minutes of irradiation is reported in **fig. 2**. Assignments were made on the basis of references [13-16].

The peak around 2964 cm^{-1} corresponds to the C-H stretching vibration. The intense band observed at 1730 cm^{-1} is assigned to the antisymmetric stretching

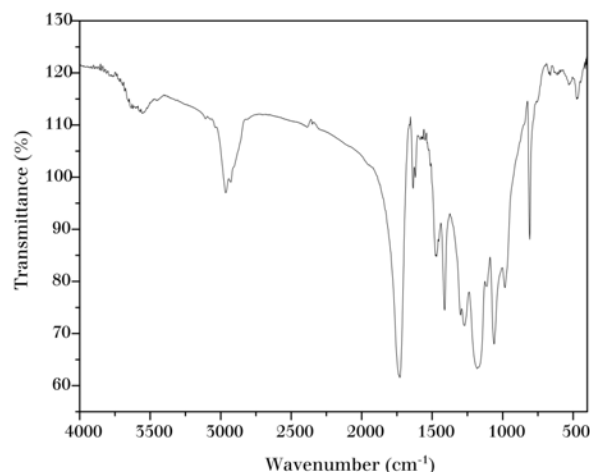


Figure 2. Infrared spectrum of a photopolymerizable resin at room temperature ($t = 20$ min).

vibration of C=O group. Bands at 1636 and 1618 cm^{-1} are assigned to the antisymmetric stretching vibration of the C=C group. The bands at 1470 and 984 cm^{-1} can be assigned to the (-CH) in-plane deformation. The bands observed between 1270 and 1060 cm^{-1} are ascribed to C-O stretching mode. The =CH₂ out-of-plane deformation appears at 808 cm^{-1} . The spectra, plotted on an absolute absorbance scale in the range of 1550 - 2000 cm^{-1} , were recorded after 4, 20 and 60 minutes of irradiation (**fig. 3**).

The reaction of photopolymerization is characterized by decrease of the C=C band intensity which is proportional to the monomer formation rate in the mixture. During the polymerization reaction, the area of band appearing at around 1618 and 1636 cm^{-1} decreases while the area of band that appears at 1730 cm^{-1} shows no evident change [14].

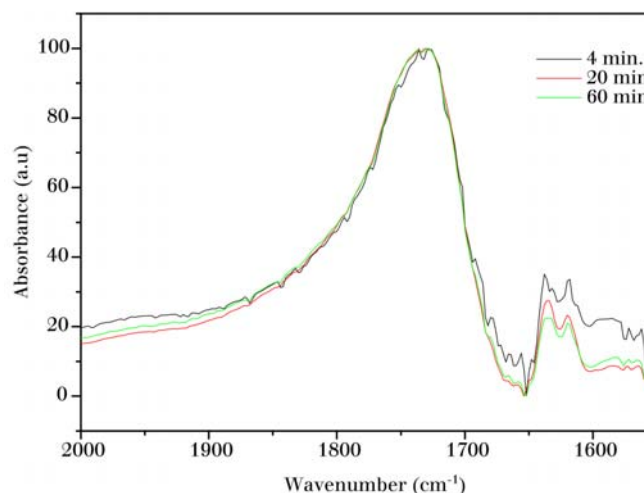


Figure 3. FTIR spectra, at the wavenumber range 1550 - 2000 cm^{-1} , of photopolymerizable resin at different irradiation times.

The C=C antisymmetric stretching vibration band, observed at 1618 and 1636 cm⁻¹, was simulated by two Lorentzian bands: The experimental data agree well with calculated predictions (fig. 4).

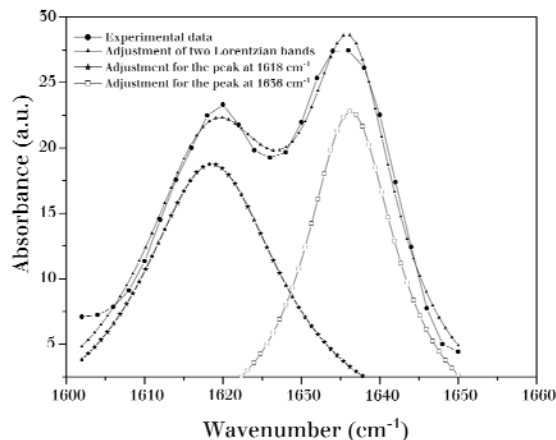


Figure 4. Simulation of the C=C band (t = 20 min).

The area of simulated bands decreased with increased light exposure time, which improved the progress of the photopolymerization reaction. Area values of simulated bands registered at several irradiation times have been evaluated and listed in table 1.

Table 1. Wavenumber at several irradiation times

Wavenumber (cm ⁻¹)	Area at 4 min	Area at 20 min	Area at 60 min
1618	1141	509	499
1636	569	560	472

Impedance spectroscopy

Figs. 5a and 5b show the complex impedance spectra of the photopolymerizable resin at several irradiation times. These spectra are characterized by the appearance of semicircle arcs whose pattern, but not shape, changes when irradiation times are raised. This pattern yields information about the electrical processes occurring within the sample and their correlation with the sample microstructure when modeled in terms of an electrical equivalent circuit [17-19]. The equivalent circuit configuration for the impedance plane plot is the resistance R_s (contact resistance), resistance R_p (polarization resistance) and in terms of complex elements: constant phase elements (capacity of the fractal interface CPE). The impedance of CPE is:

$$Z_{CPE} = \frac{1}{A_0(j\omega)^\alpha} \quad (\text{eq.1})$$

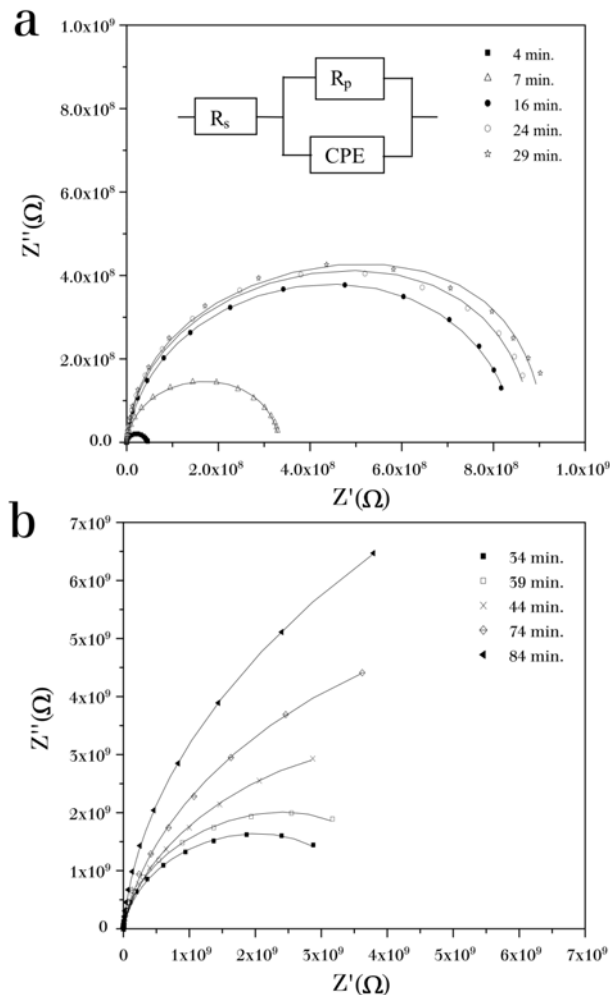


Figure 5. Impedance spectra of photopolymerizable resin for different times of photopolymerization.

Z_{CPE} is usually considered to be a dispersive capacitance, α is the measure of the capacitive nature of the element: if α=1, the element is an ideal capacitor, if α=0, it behaves as a frequency-independent ohmic resistor.

The real and imaginary components of the whole impedance of the circuit were calculated according to the following expressions:

$$Z' = R_s + \frac{R_p(1 + R_p A_0 \omega^\alpha \cos(\frac{\alpha\pi}{2}))}{(1 + R_p A_0 \omega^\alpha \cos(\frac{\alpha\pi}{2}))^2 + (1 + R_p A_0 \omega^\alpha \sin(\frac{\alpha\pi}{2}))^2} \quad (\text{eq.2})$$

$$Z'' = \frac{R_p^2 A_0 \omega^\alpha \sin(\frac{\alpha\pi}{2})}{(1 + R_p A_0 \omega^\alpha \cos(\frac{\alpha\pi}{2}))^2 + (1 + R_p A_0 \omega^\alpha \sin(\frac{\alpha\pi}{2}))^2} \quad (\text{eq.3})$$

The values of R_s and R_p can be determined from the high and low frequency limits of the measured impedance spectra, respectively:

$$R_s = \lim_{\omega \rightarrow \infty} |Z|, R_s + R_p = \lim_{\omega \rightarrow 0} |Z|$$

The parameter α can be estimated by measuring the angle between the line, which passes by centre of circle of impedance spectra and origin mark, and the real axis.

The curves of Z' and Z'' versus frequency, registered at several irradiation times, are fitted by eqs. (2) and (3), respectively. figs. 6 and 7 show the variation of Z' and Z'' versus frequency at various irradiation times, respectively, together with fits to the equivalent circuit. All fitted curves at each irradiation time shows good conformity between calculated lines with the experimental data, indicating that the suggested equivalent circuit describes the sample-electrolyte interface reasonably well.

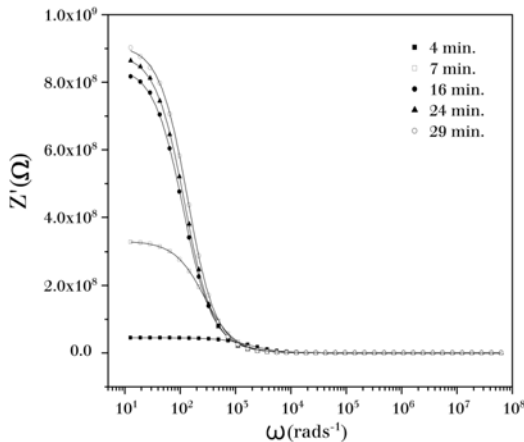


Figure 6. Variation of Z' with frequency for photopolymerizable resin at different irradiation time.

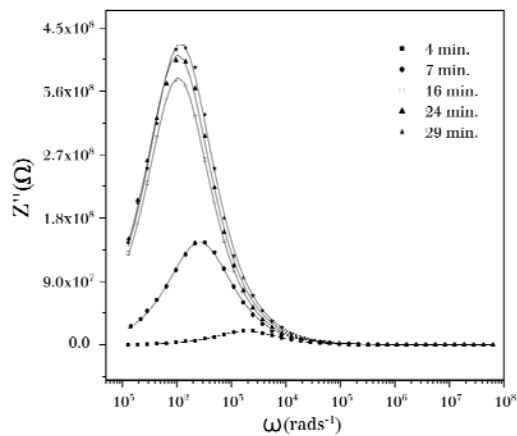


Figure 7. Variation of Z'' with frequency for photopolymerizable resin at different irradiation time.

The parameters R_p , R_s , A_0 and α have been simulated using a mean square method. All the capacitance values fell in the range of pF. The values of equivalent circuit elements have been evaluated and listed in table 2.

Table 2. Values of equivalent circuit elements

t (min)	$R_p(\Omega)10^7$	$A_0(F)10^{-11}$	α
4	4.405	1.681	0.947
7	32.38	1.241	0.960
16	77.27	1.004	0.966
24	88.38	0.989	0.967
29	91.76	0.863	0.969
34	333.4	0.777	0.970
39	403.1	0.801	0.971
44	513.3	0.975	0.964
74	801.4	0.803	0.966
84	14432	0.801	0.971

The electrical conductivity, $\sigma_p = e/R_pS$, (where S is the electrolyte-electrode contact area and e is the thickness of the sample) plotted against the irradiation time is shown in fig. 8. This figure shows a decrease of the conductivity as the photopolymerization reaction progresses: 2.11×10^{-8} and $1.16 \times 10^{-10} \text{ } \Omega\text{cm}^{-1}$ for 4 and 84 minutes, respectively. This result is correlated with the previously reported increase in viscosity [20]. Next, the change of the conductivity with an irradiation time shows two regions below and after 30 minutes. The first ($t < 30\text{min.}$), related to the monomer motion, is explained by the abundance of the monomer in this sample. After 30 minutes, the conduction imposed by the polymer became abundant with increasing irradiation times. However, all parameters remained approximately constant at great irradiation times indicating the

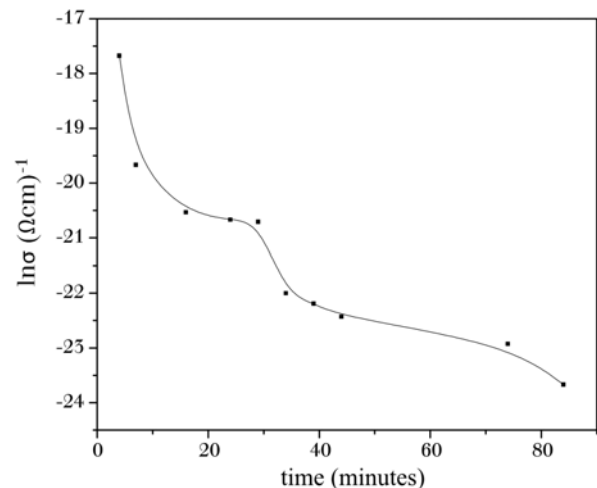


Figure 8. Irradiation time dependence of $\text{Ln}(\sigma)$.

end of the photopolymerization reaction. In fact, the IR spectroscopy study shows the decrease of the monomer abundance in sample, which can reduce the material conduction. The variation of the A_0 (fig. 9) and fractional exponent α (fig. 10) at various irradiation times confirmed the occurrence of the changes of the resistance σ_p at $t=30$ minutes.

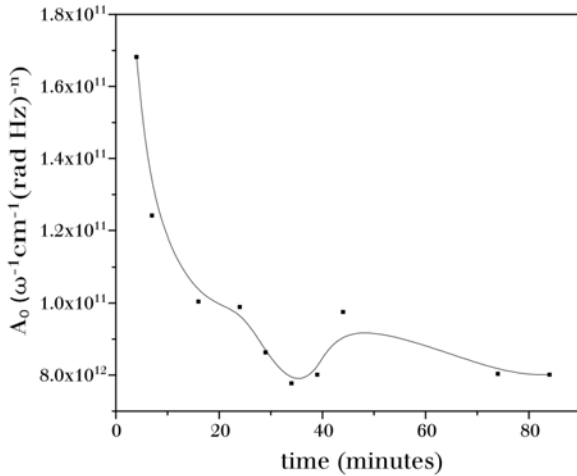


Figure 9. Irradiation times dependence of the constant phase element (A_0).

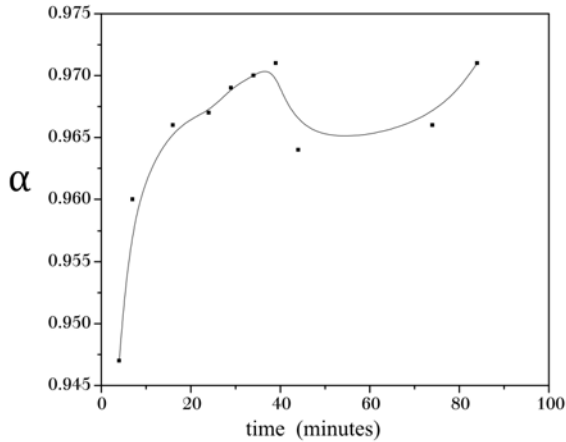


Figure 10. Irradiation times dependence of the fractional exponent α .

3.3. Modulus analysis

The modulus formalism is particularly suitable to extract phenomena such as electrode polarization and conductivity relaxation times [21,22]. The complex electric modulus can be represented by the following equation:

$$M^* = \frac{1}{\epsilon^*} j\omega C_0 Z^* \quad (\text{eq.4})$$

In this equation, C_0 is the vacuum capacitance of the cell. fig. 11 shows the variation of normalized imaginary part of the electrical modulus M''/M''_{\max} as

a function of frequency for photopolymerizable resin at several irradiation times. M''/M''_{\max} shows a slightly asymmetric peak at each irradiation times. The peak shifts toward smaller frequencies with increasing irradiation times. At the peak the relaxation is defined by the condition: $\omega_m \tau_m = 1$, where τ_m is relaxation time at the peak.

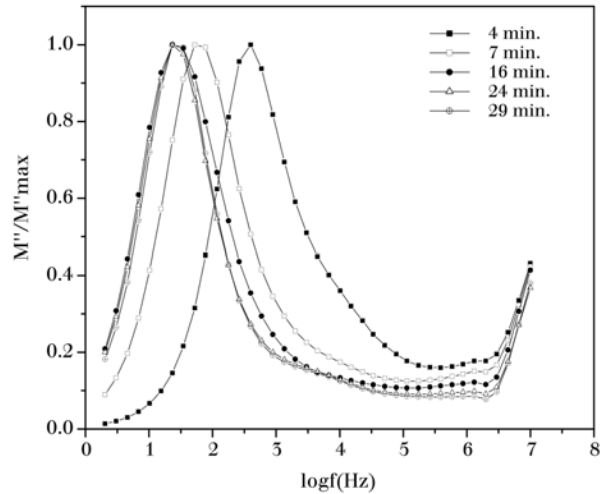


Figure 11. Plots of normalized (M''/M''_{\max}) versus $\log(f)$.

fig. 12 gives the irradiation time-dependence of the frequency relative to M''/M''_{\max} .

$$f_p = \frac{1}{2\pi\tau_f} \quad (\text{eq.5})$$

The change of the relaxation frequency f_p with an irradiation time shows two regions below and after 30 min. The first ($t < 30$ min), related to the monomer motion, and the second one connected to the polymer. This result was confirmed by impedance analysis.

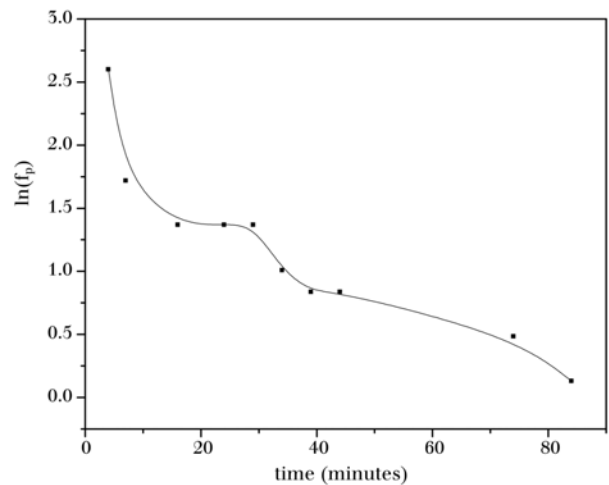


Figure 12. Dependence of $\ln(f_p)$ on Irradiation times for photopolymerizable resin.

Conclusion

In this paper, the photopolymerization and the electrical properties of the photopolymerizable resin were studied at different irradiation times. The reaction of photopolymerization was spectroscopically monitored as the decrease of the C=C band. The analysis of the frequency dispersion of the real and imaginary components of the complex impedance allowed us to determine an equivalent electrical circuit for the electrochemical cell with photopolymerizable resin. The variations of the values of the elements corresponding to equivalent circuit with irradiation time confirmed the occurrence of the change in the conductivity at 30 minutes. We attribute this to the decrease in monomer abundance in the sample.

Acknowledgements

The authors wish to thank Mourad Arous measurements of electrical impedance spectroscopy.

References

- Chang JY, Kim TJ, Han MJ, Chae KH (1999) Polymerization of N-[4-(azidocarbonyl)phenyl]maleimide and N-[4-(N'-phenoxy-carbonylamino) phenyl]maleimide: polymers containing aromatic isocyanate precursors. *Polymer* 40 (14): 4049-4054.
- Kortaberria G, Arruti P, Gabilondo N, Mondragon I (2004) Curing of an epoxy resin modified with poly (methylmethacrylate) monitored by simultaneous dielectric/near infrared spectroscopies. *European Polymer Journal* 40(1): 129-136.
- Boiteux G, Dublineau P, Feve M, Mathieu C, Seytre G, Ulanski J (1995) Dielectric and viscoelastic studies of curing epoxy-amine model systems. *Polymer Bulletin* 30(4): 441-447.
- Mangion MB, Johari JP (1991) Relaxations in thermosets. X. Analysis of dipolar relaxations in DGEBA-based thermosets during isothermal cure. *Journal of Polymer Science Part B Polymer Physics* 29(9): 1127-1135.
- Parthun MG, Johari JP (1992) Relaxations in thermosets. XVI. Dielectric studies of negative feedback during curing of an epoxide-ethylene-diamine thermoset. *Journal of Polymer Science Part B Polymer Physics* 30(655).
- Koike T (1992) Dielectric relaxation during isothermal curing of epoxy resin with an aromatic amine. *Journal of Applied Polymer Science* 44(4): 679-690.
- Senturia SD, Sheppard NF (1986) Dielectric analysis of thermoset cure. *Advances in Polymer Science* 80: 1-47.
- Carlini C, Ciardelli F, Rolla PA, Tombari E (1987). A new microwave dielectric method for studying photoinitiated chain radical polymerization processes. *Journal of Polymer Science Part B: Polymer Physics* 25(6): 1253-1261.
- Cole RH, Mashimo S, Winsor P (1980) Evaluation of dielectric behavior by time domain spectroscopy. 3. Precision difference methods. *Journal of Physical Chemistry* 84(7): 786-793.
- Livi A, Levita G, Rolla PA (1993) Dielectric behavior at microwave frequencies of an epoxy resin during crosslinking. *Journal of Applied Polymer Science* 50(9):1583-1590.
- Carlini C, Rolla PA, Tombari E (1990) Measurement method and apparatus for monitoring the kinetics of polymerization and crosslinking reactions by microwave dielectrometry. *Journal of Applied Polymer Science* 41 (3-4): 805-818.
- Tombari E, Johari GP (1992). Dielectric relaxation spectroscopy of reaction controlled slowing of molecular diffusion in liquids. *Journal of Chemical Physics* 97: 6677-6678.
- Palanisamy A, Rao BS (2006) Tetrafunctional acrylates based on β -hydroxy alkyl amides as crosslinkers for UV curable coatings. *Progress in Organic Coatings* 56(4):297-303.
- Oh SJ, Lee SC, Park SY (2006) Photopolymerization and photobleaching of n-butyl acrylate/fumed silica composites monitored by real time FTIR-ATR spectroscopy. *Vibrational Spectroscopy* 42(2): 273-277.
- Mohamed R, Razali N, Ehsan AA, Shaari S (2005) Characterisation and process optimisation of photosensitive acrylates for photonics applications. *Science and Technology of Advanced Materials* 6: 375-382.
- Choi DH, Oh SJ, Cha HB, Lee JY (2001) Photochemically bifunctional epoxy compound containing a chalcone moiety. *European Polymer Journal* 37(10): 1951-1959.
- Ben Rhaïem A, Guidara K, Gargouri M, Daoud A (2005) Electrical properties and equivalent circuit of trimethylammonium monobromodichloromercurate. *Journal of Alloys and Compounds* 392 (1-2): 68-71.
- Ben Rhaïem. A, Hlel. F , Guidara. K, Gargouri.M (2009) Electrical conductivity and dielectric analysis of $\text{AgNaZnP}_2\text{O}_7$ compound *Journal of Alloys and Compounds*).
- Nadeem M, Akhtar MJ, Khan AY (2005). Effects of low frequency near metal-insulator transition temperatures on polycrystalline $\text{La}_{0.65}\text{Ca}_{0.35}\text{Mn}_{1-y}\text{Fe}_y\text{O}_3$ (where $y=0.05-0.10$) ceramic oxides. *Solid State Communications* 134 (6): 431-436.
- Nixdorf K, Busse G (2001) The dielectric properties of glass-fibre-reinforced epoxy resin during polymerisation. *Composites Science and Technology* 61(6): 889-894.
- Almond DP, West AR (1983) Impedance and modulus spectroscopy of "real" dispersive conductors. *Solid State Ionics* 11(1): 57-64.
- Chowdari BVR, Radhakrishnan K (1989) Electrical and electrochemical characterization of $\text{Li}_2\text{O}:\text{P}_2\text{O}_5:\text{Nb}_2\text{O}_5$ -based solid electrolytes. *Journal of Non-Crystalline Solids* 110(1): 101-110.